Ammonium-Coordinated Exchanger (ACE) Functionalized Silica Sorbents for Recovering/Removing Aqueous Anionic Contaminants

Walter Chris Wilfong[a,b]; Qiuming Wang[a,b]; Fan Shi[a]; Chin-Min Cheng[a,b]; William Garber[a,b]; Karen Johnson[a,b]; Phillip Tinker[a,b]; Gita Bhandari[a,b]; Bret Howard[a]; McMahan L. Gray[a]**

[a]National Energy Technology Laboratory, 626 Cochran Mill Road, Pittsburgh, PA 15236, USA

[b]NETL Support Contractor, 626 Cochran Mill Road, Pittsburgh, PA 15236, USA

Keywords: ion exchange, sorbent, critical metal, fixed bed, silica

ABSTRACT

There are limited studies of functionalized silica anion exchange sorbents used for critical/heavy metal recovery/removal relative to polymeric and other inorganic materials. This work features ammonium-coordinated exchanger (ACE) anion exchange particle sorbents prepared by either acid-washing epoxy-crosslinked polyethylenimine (PEI) hydrogen bonded within/to a silica particle sorbent (two-step method) or reacting a di-chlorinated crosslinker, α,α-dichloro-p-xylene (DPX), with PEI within silica (single-step method). Energy dispersive X-ray spectroscopy (EDS) and infrared spectroscopy confirmed the presence of $-NH_2^+\cdots Cl^-$ and $-NH_3^+\cdots Cl^-$ groups, which removed oxyanionic species –arsenate, selenate, chromate, sulfate, phosphate, and nitrate– plus bromide from ideal solutions, authentic acid mine drainage (AMD), and authentic flue gas desulfurization (FGD) wastewater. Affinity of the anions for ACE varied across single- and mixed-element solutions. However, affinity for CrO_4^{2-} was among the highest in both cases. Total anion uptake by the optimized ACE, PEI-E3-HCl_1.1, reached 1.2 mmol anion/g-sorb. (0.56 mmol CrO_4^{2-}/g), or ~2.3 mmol negative charge/g-sorb.. This was close to that of a commercial anion exchange resin (0.52 mmol CrO_4^{2-}/g). Near-consistent removal of 20-80% of each anion from FGD during an eight-cycle adsorption-desorption (1M NaCl) test predicted good ACE viability for testing under practical conditions at larger scale.

1. INTRODUCTION

The U.S. Resource Conservation and Recovery Act (RCRA) endowed the U.S. Environmental Protection Agency (EPA) with the authority to establish and enforce regulatory policies and toxicity limits regarding Arsenic (As), Cadmium (Cd), Chromium (Cr), Lead (Pb), Mercury (Hg), Selenium (Se), and other metals because of their potential harmful effects on human health.[1] Capturing Se, As, and Cr is particularly challenging because they are commonly present in polyatomic oxyanion forms. These forms can vary in chemical structure, influenced by factors

such as solution pH and oxidation-reduction reactions with different organic (e.g., microbes) and inorganic (e.g., iron oxide) constituents in the water.[2-5] As and Cr were also deemed Critical Minerals/Metals by the U.S. Geological Survey largely because of the U.S.'s reliance on foreign sources for these vital elements. Notably, 100% of the U.S. demand for As is supplied by China while 74% of the demand for Cr originates from South Africa.[6] Serendipitously, two key focuses of the U.S. Department of Energy's (DOE) research efforts are the removal and recovery of heavy and critical metals from waters, particularly if the heavies originate from a fossil-related contamination source.

Sources containing the more toxic species are usually industry-related, including runoffs from flue gas desulfurization (FGD) wastewater,[7] acid mine drainage,[8] and other processes. The EPA 2020 Steam Electric Reconsideration Rule, an update to the 2015 regulation, instituted concentration limits for a series of contaminants including As, Se, NO_3^-/NO_2^-, bromide, Br^{-1}, and Hg. Anionic NO_3^- and NO_2^- species are further regulated by the EPA for their role in producing acute but reversible health effects if consumed. Some sources for these contaminants can be natural, such as fertilizer/agricultural runoff containing excess nitrate and phosphate.[9] Although not as harmful as the RCRA species, sulfate(SO_4^{2-}) can pose problems such as cracking of cement and brick mortar, and corrosion of copper piping in residential homes and industry. Furthermore, the EPA issued an advisory for sulfate due to its laxative effect and because it reduces the taste and odor aesthetics of drinking water.

Common methods to mitigate toxic or nuisance metals include electrocoagulation, phytoextraction, advanced oxidation processes, biological remediation, membrane separation, and adsorption, with ion exchange being a large subset.[10-12] These methods are also commonly used for the recovery of critical metals. Adsorption-based remediation methods are particularly easy to scale, especially ion exchange processes which are commercialized and routinely used to treat contaminated industrial water.[13] Commercial ion exchange materials typically include functionalized organic polymers, such as modified crosslinked styrene-divinylbenzene; organic-inorganic hybrids like chitosan-modified organoclay[14], ionic covalent organic frameworks[14], or others where polymers are combined with metal oxides or metal hydroxides; and bare zeolites.[15-18] Although commercialized, polymer-based ion exchange resins have notable drawbacks, including the need for complex synthesis via emulsion or suspension polymerization, susceptibility to swelling and fracturing during operation with potential contributions to the microplastic pollution, and oxidation issues especially for OH^- forms.

Contrasting the resins, functionalized silica sorbents represent a subclass of organic-inorganic hybrid material that can be synthesized in one simple and scalable step through dry or wet impregnation methods.[19] The combined low cost, high mechanical strength, and chemical tunability of silica avail a plethora of robust formulas customized to suit different water chemistries. Traditionally, silica was functionalized primarily with chelating agents, such as crosslinked polyamines, like polyethylenimine;[20, 21] aminosilanes, including 3-aminopropyl triethoxysilane;[22] diglycolamide-type ligands (ex. diglycol-2,4-diamido-propyltriethoxysilane);[23] tetradentate phenylenedioxy diamide-type ligands (ex. 1,2-phenylenedioxy diamido-propyltriethoxysilane);[24] carboxylic acid-based ligands, like ethylenediaminetetraacetic acid[25] and N, N-dioctyldiglycolic acid[26]; phosphate-based ligands, like diethylphosphatoethyltriethoxysilane;[27] and many others for cationic lanthanide and transition

metal removal. However, these chelation-based formulas are less effective or fail at capturing anions like selenate, chromate, sulfate, and more. Still, research into silica-supported anion exchanger material remains relatively limited, despite their potential to overcome these limitations and broaden removal capacities.[28-36]

Herein, we describe ammonium-coordinated exchanger (ACE) crosslinked functionalized silica sorbents that behave as anion exchangers and are suitable for water treatment and critical metal recovery. These ACE leverage an ammonium-chloride anion exchange mechanism, significantly enhancing the removal of oxyanion contaminant or critical species from industrial wastewaters compared to conventional chelation-based sorbents. The ACE material demonstrated superior performance over a well-established commercial anion exchange resin in both synthetic and authentic water sources, underscoring its effectiveness for the removal and recovery of target species.

2. EXPERIMENTAL

2.1 Materials

Reagents used to prepare sorbents were the following: branched polyethylenimine with molecular weight 800 g/mol (PEI, Millipore Sigma); N-N-diglycidyl-4-glycidyloxyaniline (E3, Millipore Sigma); methanol (HCl, certified ACS, Fisher Chemical); silica (500 μm particle size, PQ CS 2129, PQ Corp. or 600 μm particle size PPG Flo-Gard 214); HCl (certified ACS Plus, Fisher chemical); H_2SO_4 (ACS reagent, 95.0-98.0%, Sigma-Aldrich); and α,α-dichloro-p-xylene (DPX, 98%, Millipore Sigma). Metal salts used to prepare standard metal uptake solutions were the following: Na_2SO_4 (ACS reagent, ≥99.0% anhydrous, granular, Sigma-Aldrich); Na_3PO_4 (95%, Sigma-Aldrich); $NaNO_3$ (≥99.0%, Sigma-Aldrich); $NaCrO_4$ (98%, Sigma-Aldrich); Na_2HAsO_4 (heptahydrate form, ≥98.0%, Sigma); Na_2SeO_4 (≥95%, Sigma-Aldrich); and NaCl (Fisher, certified ACS). The gas used to perform CO_2 capture experiments with the sorbents was 100% CO_2 (industrial grade, Butler).

2.2 Sorbent Preparation

An array of immobilized amine sorbents comprised of 30-40 wt.% organic species on silica (SiO_2) were prepared by dissolving 1.6-3.5 g amounts of PEI and 0.5-2.4 g tri-epoxide monomer, E3, in 100 g MeOH. Each resulting impregnation solution was then mixed with 6.0 g of silica in a 250 mL round-bottom flask. The flask was placed in a rotary-evaporator and heated at 60 °C while rotating at 100 rpm and sequentially pulling a vacuum of 0.27 to 0.96 bar for 60 min to evaporate methanol. Additional heating in either the rotary evaporator under slight vacuum or in the oven at 90 °C for 30-60 min ensured sufficient crosslinking occurred. The nominal amount of E3 on the final sorbent was 4.6-24 wt.% and PEI was 16-35 wt.%, giving E3/PEI weight ratios between 0.13 and 1.50. These are assumed the same ratios as those of the starting impregnation solutions.

The dried sorbents were screened for their water stability via accelerated water washing as reported elsewhere.[37] Approximately 0.5 g non-protonated sorbent were placed in a packed bed; 20 mL ultrapure Milli-Q water were passed at 0.5 mL/min over the sorbent. Then, the organic content of the washed sorbent was determined by TGA decomposition runs. Upon determining the most water-stable formula, the remainder of that sorbent was washed in a batch setup. Approximately 5.0 g of the sorbent were soaked in multiple batches of fresh ultrapure Milli-Q

water under gentle tumbling until the leached non-crosslinked PEI concentration in water was less than 50 ppm, approximately 1,500 ml water for 5.0 g dry sorbent. The PEI concentration was determined by a ultraviolet-visible light (Uv-VIS) Cu^{2+} spectrometric method, as reported in our previous work.[38] Briefly, amine wash solution samples were diluted with ultrapure water; 2 mL wash solution was mixed with 2 mL 500 ppm Cu^{2+} solution; then the mixture was scanned in a GENESYS IS 10 (Thermo Scientific) ultraviolet-visible spectrometer to determine aqueous amine concentration.

After H_2O washing, the sorbent was filtered then treated in a batch setup with either 0.1 M HCl, pH 1.1 or 0.1M H_2SO_4, pH 1.7 solution by soaking the water-washed sorbent in one to three, 500 mL acid portions until the pH of the treated solution was nearly equal to that of the fresh acid solution. Acid-treating pre-synthesized amine sorbents represented a two-step preparation process for the ACE. After acid treatment, each sorbent was filtered and washed with copious amounts of ultrapure water until the pH of the liquid was 3 to 4, and then was dried at 60 °C overnight. Treating the washed sorbent with low pH acid caused protonation of the amine groups to generate primary, secondary, and possibly tertiary ammonium ions interacting with the Cl^- of HCl and SO_4^{2-}/HSO_4^- of H_2SO_4. These ionic species serve as exchangeable groups that are displaced by toxic anion species which become adsorbed through ionic interactions with the ammonium ions. The sorbents are labeled as PEI-E3/S-HCl_X, where X is the pH value of the soaking solution.

An array of single-step ACE comprised of organic species on silica were prepared by first separately dissolving different amounts of PEI in MeOH warmed on a hotplate set at 50-60 °C. Next, various amounts of a dichloro-based linker, DPX, were dissolved in each of the warm PEI/MeOH solutions. The resulting impregnation solutions were then mixed with 6.0 g portions of silica (600 μm, PPG Flo-Gard 214) in 250 mL round-bottom flasks. Each flask was placed in a rotary-evaporator then heated to dry and the sorbent was cured similarly as the amine sorbent from the two-step process. A total of six single-step sorbents were prepared with the following nominal mol Cl/mol N ratios – 0.6, 0.8, 1.0, 1.2, 1.4, and 1.6. Subsequently, the dried sorbents were washed with water then MeOH to remove unbound organics and were then dried again. The sorbents were denoted as, PEI-DPX/S-Y, where Y was the Cl/N molar ratio. A scheme of the preparation processes for the single-step and two-step methods is shown in Scheme S1 of the supporting information.

2.3 Characterization

Infrared Spectroscopy

Diffuse Reflectance Infrared Fourier Transform Spectroscopy (DRIFTS) analysis was performed on the as-is and protonated sorbents to assess the sorbents' chemical structures resulting from interaction with the acid. Approximately 10-50 mg of sorbent were loaded into the sample cup of a DRIFTS SMART accessory set inside a Nicolet 8700 infrared spectrometer (ThermoScientific). Infrared (IR) single beam spectra of pretreated sorbents (120 °C, N_2, 30 min) were obtained at 50 °C from 50 co-added scans collected over 30 s at a 4 cm^{-1} resolution.

Scanning Electron Microscopy (SEM) and Energy Dispersive X-Ray Spectroscopy (EDS)

SEM images (not shown) of fresh and ACE sorbents were obtained with an FEI Company Quanta 600 field emission SEM equipped with secondary and backscatter electron detectors. EDS

elemental assessment of N, Cl, and S of the sorbents observed by SEM was accomplished with an Oxford Inca Energy 350 X-act EDS analyzer.

Carbon-Hydrogen-Nitrogen-Sulfur Analysis

Carbon-hydrogen-nitrogen-sulfur (CHNS) analysis of the original and acid washed sorbents was performed with a Perkin Elmer II Series CHNS elemental analyzer to determine the N and S content of the materials. Generally, solid sorbents were combusted in an oxygen-rich environment, where the generated gases were analyzed with a frontal chromatography unit.

Contaminant Anion Adsorption Studies

Metal uptake tests with the ACE were conducted primarily at room temperature, 20-22 °C, by either flow or batch mode. Details can be found in the supporting information, wherein Tables S1 and S2 show the composition of solutions tested in this work.

Thermogravimetric Analysis - CO_2 Adsorption and Organic Loading

Thermogravimetric analysis (TGA, TA instruments model 5500) CO_2 adsorption runs were conducted on the sorbents to characterize the non-protonated/free amine remaining after sorbent preparation that can capture CO_2. Conversely, protonated amines are inactive toward CO_2 due to the interaction of the N lone electron pair (CO_2 capture site) by the bonded hydrogen atom. Sorbents were first pretreated for 30 min at 105 °C in 25 mL/min flowing N_2, then were cooled down to 50 °C and exposed to 25 mL/min flowing 100% CO_2 (industrial grade) for 2 hours.

TGA decomposition studies of the fresh and some washed sorbents were performed to determine their organic loading in weight percentages, using the follow procedure: heating at 105 ºC in flowing N_2 to remove CO_2 and water pre-adsorbed from the environment; switching the flow to air; jumping to 800 ºC and holding for 10 min; then cooling.

Hydrogeochemical Modeling

The distribution and chemical speciation of the tested oxyanions as a function of pH were calculated using PHREEQC software (Version 3.7.3), provided by the U.S. Geological Survey. The calculation was done by conceptualizing a titration process in which 5 mM of a selected Na-oxyanion solution, i.e., Na_2HAsO_4, Na_2SO_4, Na_3PO_4, $NaNO_3$, and Na_2SO_4, was titrated with HCl from pH 12 to approximately pH 1. The interference of CO_2 is neglected. For CrO_4^{-2}, the speciation distribution was calculated at the three specified Eh-pH conditions measured from the solutions. The Eh-pH diagrams depicting the dominant aqueous species at a defined Eh-pH range were constructed by PhreePlot (Kinniburgh and Cooper, 2004). The Lawrence Livermore National Library (LLNL) database was used for both PHREEQC and PhreePlot calculations.

3 RESULTS

3.1 ACE Characterization

Table 1 shows the composition of each ammonium-coordinated exchanger sorbent, prepared by either the two-step/acid washed method or the single-step method. Average Cl/N and S/N (H_2SO_4 washed) ratios for the sorbents were determined by EDS mapping of multiple particles, as shown in Table S3 of the SI. Figure 1 (a) shows the DRIFTS spectra of the PEI-E3/S-HCl_X two-step ACE sorbent samples, prepared by soaking the starting crosslinked sorbent overnight in HCl

solutions at pH values from 1-7. Soaking in near-neutral solution (~pH 7, H_2O-washed control) expectedly did not protonate the amines to form ammonium ions, as observed from our previous work.[39] Beginning at pH 4.3, the IR spectra of the HCl-soaked sorbents revealed subtle broadening of the N-H stretching features for $-NH_2^+/-NH_3^+$ between 3,600 and 3,000 cm^{-1} and approximately 2,480 cm^{-1}.[40] These spectral changes indicate the onset of ammonium ion formation, confirming amine protonation under increasingly acidic conditions.

Table 1: Composition of two-step acid washed and single-step ACE sorbents.

Sorbent	Loading, Washed (wt.%)	Avg. mmol Cl, S/g-sorb. (STD)	Avg. Cl/N (or S/N) Ratio, Washed[a]	OCR, Fresh (wt.%)[b]
PEI-E3/S	30.8	0.09 (0.02)	0.019	102.4 (TGA), 91.5 (CHNS)
PEI-ES/S	28			94
PEI-E3/S-HCl_5.9	31.8	0.08 (0.04)	0.013	-
PEI-E3/S-HCl_4.3	36.5	0.06 (0.02)	0.01	-
PEI-E3/S-HCl_3.2	34.8	0.67 (0.22)	0.12	-
PEI-E3/S-HCl_2.1	37	1.27 (0.12)	0.22	-
PEI-E3/S-HCl_1.1	39.1	1.29 (0.60)	0.24	-
PEI-E3/S-H_2SO_4_1.7		1.1 (0.26)	0.25	
PEI-ES/S-HCl				
PEI-DPX/S_0.6	29.6	0.50 (0.11)	0.07	81.2
PEI-DPX/S_0.8	31.1	0.69 (0.24)	0.14	112
PEI-DPX/S_1.0	31.9	0.77 (0.13)	0.15	99.6
PEI-DPX/S_1.2	29.4	0.77 (0.17)	0.16	86.2
PEI-DPX/S_1.4	23.7	-	-	90.4
PEI-DPX/S_1.6	21.8	-	-	80.2

a. Determined by EDS. Standard Deviations from the average are shown in Figure 1; b. OCR - organic content returned=Organics,wt.%$_{washed}$/Organics,wt.%$_{fresh}$ x 100%. Although inorganic, HCl coordinated to the sorbent is considered part of the sorbent organics loading.

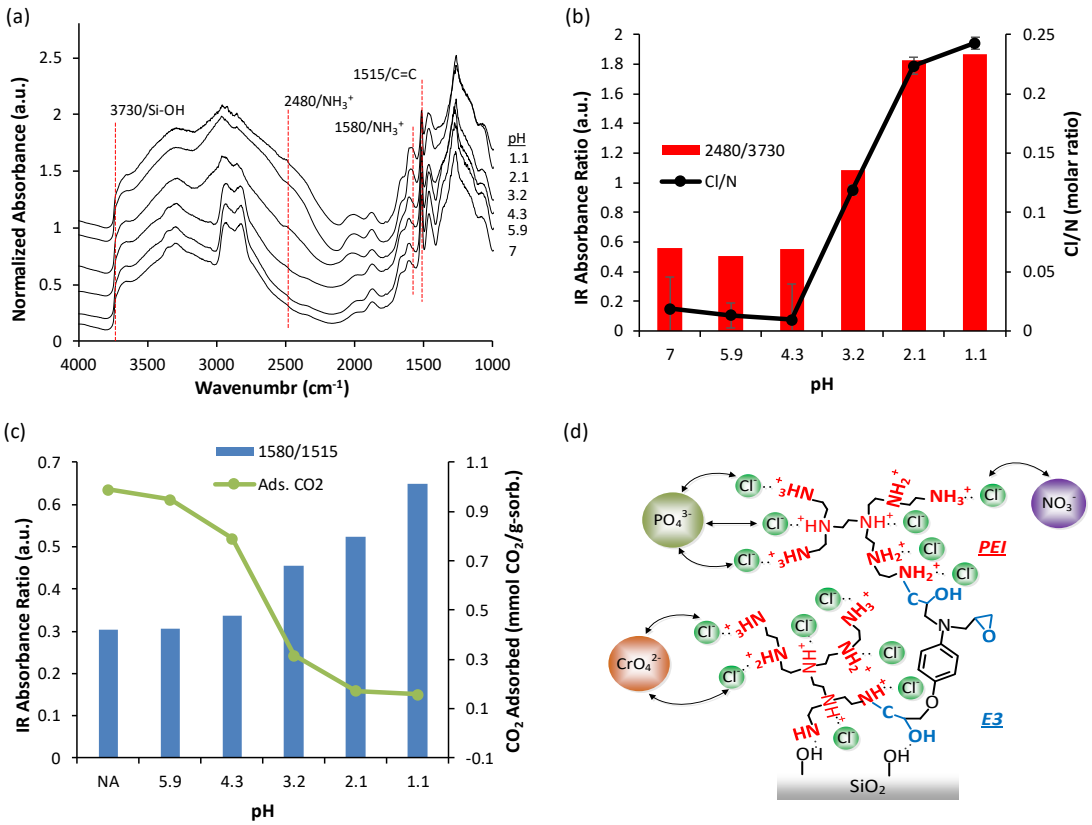

Figure 1: (a) Normalized IR absorbance spectra (absorbance=log (1/intensity)) of the two-step ACE sorbents prepared with different pH values of HCl solution. Intensities of the spectra were normalized from 0 to 1; (b) and (c) effect of pH/HCl concentration on ammonium ion formation, EDS Cl/N ratio, and CO_2 adsorption capacity. EDS Cl/N molar ratios are averages of 5-8 measurements across the particle surface. "NA" represents the PEI-E3/S sorbent that was not acid-washed. (d) One theoretical representation of the two-step ACE sorbent structure and the sorbents' anion exchange behavior.

Dropping the pH to 3.2 and below protonated the amines and generated appreciable $-NH_2^+/-NH_3^+ \cdot Cl^-$ pairs within the sorbents, signified by the disappearance of the amine stretching doublet; substantially broadened ammonium ion N-H stretching features; and the generated N-H stretching band at 1,580 cm^{-1}. Corresponding suppression of the C-H stretching bands at 2,935 and 2,820 cm^{-1} further confirmed the formation of ammonium ions.[41, 42] Ammonium-carbamate ion pairs from adsorbed CO_2 on immobilized amine CO_2 sorbents produce similar N-H IR features as those of the ammonium-chloride pairs observed here.[42, 43] Figure 1 (b) further confirms the presence of ammonium ions as ammonium-chloride pairs by plotting the 2480/3730 absorbance ratio alongside the EDS Cl/N molar ratio against pH. Here, the Si-OH band at 3,730 cm^{-1}, which remains unaffected by acid washing, serves as an internal reference. Both the 2480/3730 ratio and the EDS Cl/N ratio show minimal change down to pH 4.3, whereafter starting at pH 3.2, both profiles rise sharply, indicating increased ammonium ion formation.

Because ammonium ions are inactive to chemisorbing CO_2, the CO_2 uptake of the HCl-washed sorbents decreased as the free amines were converted to the protonated forms, as shown in Figure

1 (c). The 1580/1515 (C=C, E3, internal reference) plot here highlights the consistency in the results when using different ammonium ion and internal reference IR bands. Leveling-off of nearly all profiles in (b) and (c) suggests the amines reached maximum protonation under the preparation conditions. However, at the lowest pH (1.1), only an 84.2% reduction in CO_2 capture down to 0.17 mmol CO_2/g was observed. This residual uptake indicates the presence of unprotonated free amines, likely confined within the inner sorbent pores, whose IR signatures are obscured by the broad ammonium ion features near the pore mouth and on the particle surface. The presence of free amines aligns with findings from previous studies that early-stage amine protonation inhibited further protonation of tertiary amines due to electrostatic suppression.[44] Others observed a similar phenomenon when titrating tetraethylenepentamine with HCl.[45] Branched PEI_{800} used here was reported to have 41.9% -NH_2 (primary), 35.0% -NH (secondary), and 23.1% -N (tertiary) amine groups.[46] The maximum Cl/N ratio for the pH 1.1 washed sorbent shows that only 24.3% of all amines are ammonium-chloride ion pairs. The ammonium-chloride and free amine species gave the ACE both anion exchange, as shown in (d), and chelation metal uptake mechanisms. Overall, the results show that an optimal ammonium-coordinated chloride anion exchange sorbent was PEI-ES/S-HCl_1.1 prepared at the lowest pH. This ACE sorbent will be used for all further anion exchange tests involving the PEI-E3/S-HCl_X formula type.

Potentiometric titration of the PEI-E3/S-HCl_1.1 sorbent with 0.1 M NaOH, shown in Figure 2, reveals four pKa values – 2.9, 4.9, 6.9, and 9.9. These pKa values are similar to those reported elsewhere for PEI and aliphatic amines that resemble segments of the PEI molecule.[44]

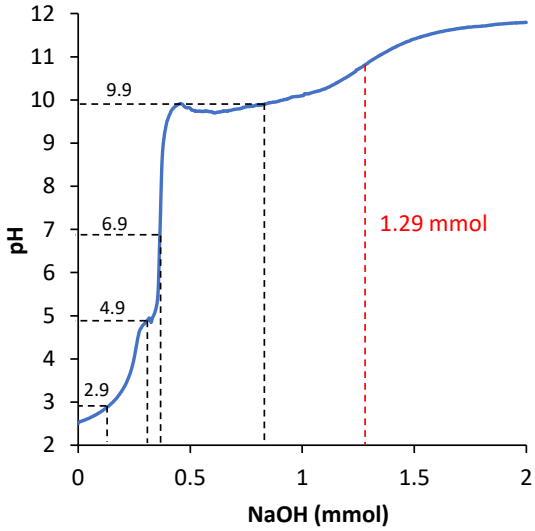

Figure 2: Potentiometric titration of 0.5 g two-step PEI-E3/S-HCl_1.1 with 0.1 M NaOH.

The lowest 2.9 pKa is close to the pH at which PEI was appreciably protonated by HCl, as demonstrated in Figure 1. The highest pKa 9.9 represents the upper pH limit at which the sorbent still maintained at least one-half of its remaining ammonium-chloride groups between the third and fourth equivalence points. A total of 1.29 mmol NaOH (2.58 mmol NaOH/g-sorb.) were required to neutralize all ammonium-chloride groups, indicating that the maximum uptake capacity of the sorbent is ~2.6 mmol negative charge/g-sorb.

3.2 ACE Metal Uptake from Ideal Solutions

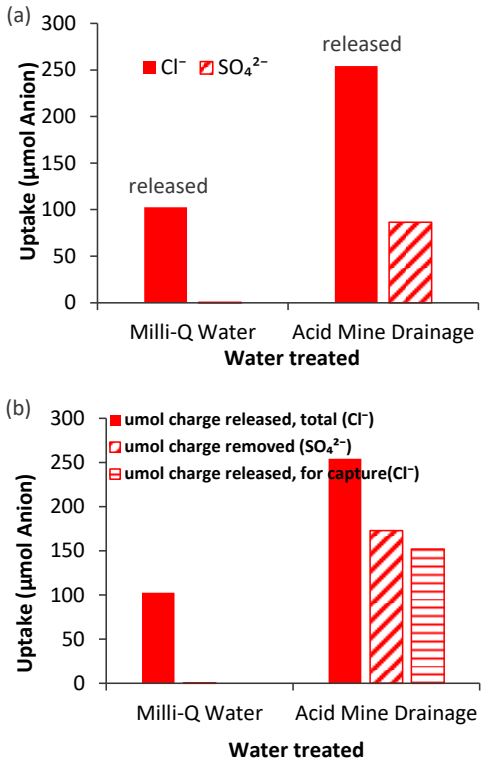

Figure 3: Sulfate uptake from authentic acid mine drainage, reported by both (a) µmol anion and (b) µmol negative charge bases. Chloride release from leaching of weakly bound HCl was also determined by soaking the two-step ACE sorbent in RO water. Conditions: 0.5 g PEI-E3/S-HCl_1.1; AMD, 20 mL, 0.5 mL/min; pH 3.4; 22 °C.

Figure 3 (a) shows the explicit uptake of SO_4^{2-} from authentic AMD and the implicit leaching of non-bound HCl into the RO water control under flow conditions. Sulfate was the only prevalent anion of all those analyzed for and found in AMD, at 202 mg/L. The 0.5 g PEI-E3/S-HCl_1.1 sample removed 86.4 µmol SO_4^{2-} while releasing 254 µmol Cl^- upon treating 20 mL AMD. Both re-calculating the Cl^- released to account for its loss as leached HCl and converting from a µmol anion to a µmol negative charge basis in (b) gives 172.8 µmol charge removed as SO_4^{2-} and 152 µmol negative charge released as Cl^{-1}. The 0.88/1 charge ratio of Cl^-/SO_4^{2-} results here strongly support the exchange behavior of PEI-ES/S-HCl_1.1 to remove anionic contaminants from water. Two nearby chloride 1- anions are exchanged for one sulfate 2- anion.

Figure 4 compares the relative maximum uptake of CrO_4^{2-}, $HAsO_4^{2-}$, SeO_4^{2-}, SO_4^{2-}, NO_3^-, and HPO_4^{2-}/PO_4^{3-} from (a) single- and (b) mixed-element solutions. These tests involved either one or both the chloride and sulfate forms of the two-step ACE, the precursor immobilized amine sorbent, commercially available ion exchange resin A600E/9149, and activated carbon. The dominant oxyanion species were determined from the speciation model calculations presented in Figures S1 and S2 in the supporting information. As shown in Figure 4 (a), AC displayed minimal to no anion uptake due to its predominantly aromatic structure which contains scattered oxygen-containing groups (e.g., carboxylic acids, hydroxyls, and carbonyls).[47] None of these groups adsorbed species through anion exchange, confirming that AC's adsorption mechanism does not involve ion exchange processes.

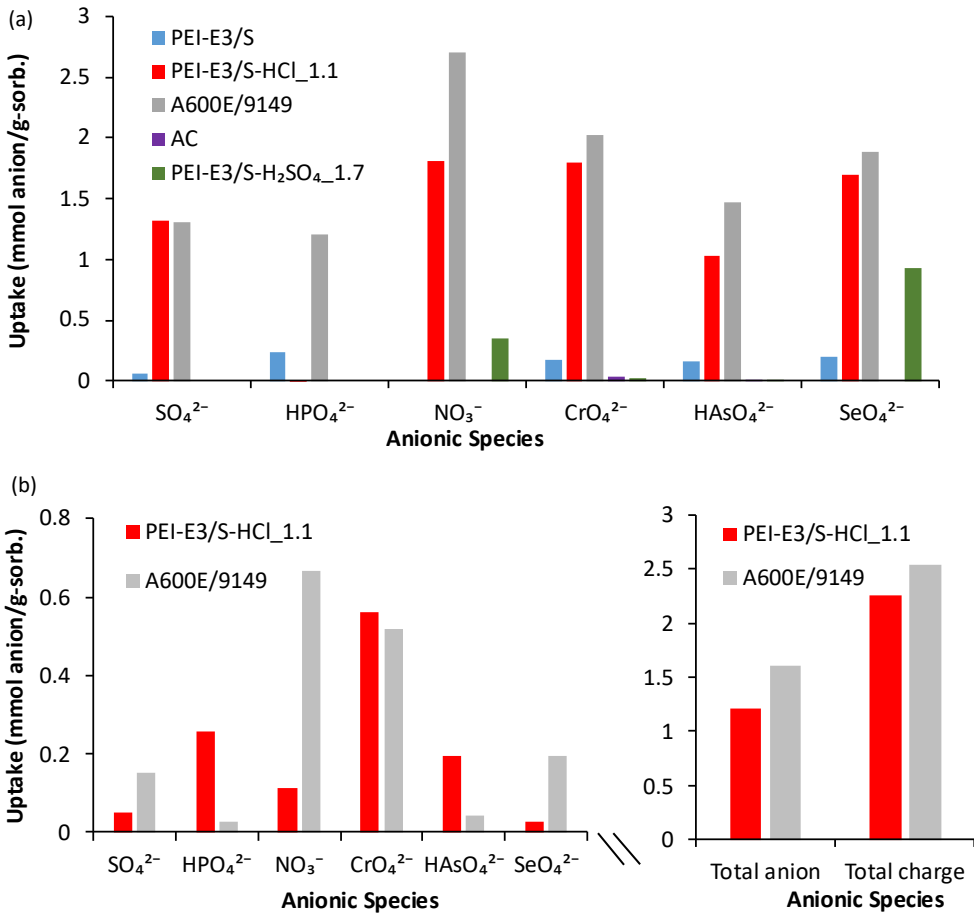

Figure 4: Comparison of relative maximum uptake capacities of anions by two-step ACE, immobilized amine sorbent, anion exchange resin, and activated carbon from approximately 5 mM total concentration (a) single-element i-iv and (b) mixed-element ii solutions. The inset numbers in (a) represent the initial pH of each solution. Conditions: 0.05 g PEI-E3/S-HCl_1.1; ~5 mM total, equimolar anions for (b) (except 2.5 mM NO_3^- in (b)), 50 mL, 24 hours; pH 5.5-12; 22 °C.

Minimal adsorption of the anions by the crosslinked PEI sorbent suggests inefficient chelation by the lone electron pairs of PEI nitrogen groups due to the anions' negative charge. Conversely, PEI-E3/S-HCl_1.1 with ammonium-chloride ion pairs adsorbed appreciable amounts of anions in terms of mmol anion/g-sorb. as: CrO_4^{2-} (pKb 7.5 – pKb=14-pKa of protonated form ($HCrO_4^-$)), NO_3^- (pKb 15.3)>SeO_4^{2-} (pKb 12.1)>SO_4^{2-} (pKb 12)>$HAsO_4^{2-}$ (pKb 7.2)>> HPO_4^{2-} (43.5%)/PO_4^{2-} (53.5%), none (pKb 6.8 and 1.7).[48] Excluding CrO_4^{2-}, which also participated in oxidation-reduction reactions, oxyanion affinity of the ACE increased with decreasing basicity, increasing pKb values. It was described that low basicity anions (high pKb's/low pKa's) interact weakly with water and have lower hydration energies, and therefore are more amenable to occupying the internal anion exchange resin matrix than outside it. Therein, the counter-anions and resin matrix interfere with organized water structures, which themselves are found outside the resin and provide a stable environment for higher basicity anions (lower pKb's) having greater hydration energies.[49] Importantly, CrO_4^{2-} and SO_4^{2-} followed this trend by having $\Delta G_{hydr.}$ values of -950 and -1,080 with corresponding pKa values of 6.5 ($HCrO_4^-$) and 2 (HSO_4^-), respectively.[50] This supports that a

mechanism beyond pure ion exchange, like oxidation-reduction, is responsible for the superior performance of the ACE toward the Cr species.

PEI-E3/S_H_2SO_4-1.7 recovered only NO_3^- and SeO_4^{2-}, significantly underperforming its Cl^- based counterpart. Because each lone electron pair of PEI N-groups can accept one proton, depending on the pH of the solution, -NH_2^+/-$NH_3^+ \cdot HSO_4^-$ (protonated by H_2SO_4, pKa -4.8/HSO_4^- pKb 18.8) and -NH_2^+/-$NH_3^+ \cdot SO_4^{-2} \cdot {}^+{}_3$HN-/$^+{}_2$HN- (protonated by HSO_4^- pKa 2.0/SO_4^- pKb 12) are expected to be the ion pairs for PEI-E3/S_H_2SO_4-1.7.[51] The former species is expected to be the dominant form. The lower pKb (18.8, higher basicity) for HSO_4^- than for 17.9 for $C1^-$ suggests stronger binding of the former to the ammonium ions, and hence its inferior ion exchange ability.

The A600E/9149 resin outperformed the Cl^- form ACE to varying degrees for the uptake of most anions, except for SO_4^{2-}, regarding the single-element solutions and displayed a somewhat similar trend in anion affinity as the PEI-E3/S-HCl_1.1. As shown in Table 2, the PEI-E3/S-HCl_1.1 sorbent demonstrated competitive performance with A600E/9149 for the removal of critical metal Cr and/or other anions from ideal solutions. Additionally, the performance of PEI-E3/S-HCl_1.1 sorbent surpassed that of other ACE-based sorbents reported in the literature, highlighting its efficacy in critical metal recovery and water treatment applications.

Table 2: Literature survey of different ammonium-coordinated exchanger sorbents used for the removal of Cr and other anions from water.

Ion Exchange Sorbent	Description	Contaminant	Conditions	Uptake	Ref.
SiPyR-N4	Crosslinked 4-pyridine-divinylbenzene/silica, Cl^- form	ReO_4^-	Batch, 25 °C, pH 7.6, 500 mg/L, 0.05 g-sorb./20 mL	0.85 mmol ReO_4^-/g	29
MS-76-NH_3^+-G	Protonated 3-aminopropyltriethoxysilane/silica, Cl^- form (HCl washed)	NO_3^-, $H_2PO_4^-$	130 mg NO_3-($NaNO_3$) and 100 mg/L $H_2PO_4^-$ (NaH_2PO_4), 0.05 g-sorb./50 mL, 3 hrs	0.70 mmol NO_3^-/g-sorb, 0.55 mg $H_2PO_4^-$/g-sorb	30
SBA15Im0.25Cl-3h	1-Methyl-3-(triethoxysilylpropyl)imidazolium chloride/silica, Cl^- form	Cr (VI)	Batch, 25 °C, pH 4.6, 0.01 g-sorb./15 mL, 60 mg Cr/mL, 1 hrs	1.74 mmol $HCrO_4^-$/g	31
QPEI-ZrO_2	Quatenized, crosslinked 1,4-butanediol diglycidyl ether PEI/zirconia (HCl washed)	NO_3^-	Chromatography, flow, 35 °C, pH 7.4, 1 mL/min, 5 uL inj., 10 mM	capacity factor, k'=1.48	52
Amberlite® IRN-78,	PS-DVD strongly basic gel-type anion exchange resin, OH^- form	CrO_4^{2-}	Batch, 0.05 g sorb./20 mL, 1.15-2.0 mmol/L Na_2CrO_4, 25 °C	0.9 mmol CrO_4^{2-}/g	53

PSi.1ANEX1	Crosslinked poly(vinylbenzyl chloride)-N,N,N',N'-tetramethyl-1,2-ethylenediamine/silica	CrO_4^{2-}	Batch, isotherm (to 750 mg/L), 1 g sorb./L, pH 4, 23 °C, 6 hrs	1.6 mmol Cr(VI)/g (langmuir)	[36]
A600E/9149	PS-DVD strongly basic gel-type anion exchange resin, Cl^- form	CrO_4^{2-}	Batch, 50 mg sorb./50 mL, pH 7.7, 23 °C, 24 hrs	2.0 mmol CrO_4^{2-}/g	This work
PEI-E3/S-HCl_1.1	Epoxy-crosslinked polyethylenimine/silica, Cl^- form (HCl washed)	CrO_4^{2-}	Batch, 50 mg sorb./50 mL, pH 7.7, 23 °C, 24 hrs	1.8 mmol CrO_4^{2-}/g	This work

PEI-E3/S-HCl_1.1 exhibited different anion uptake behavior in the mixed-element compared to the single-element solution, due to factors such as competitive anion adsorption and complex anion-anion interactions. The most notable change was the adsorption of phosphate species and the increased ratios of adsorbed CrO_4^{2-} to all other anions. The pH 11 mixed solution was calculated to have a higher ratio of HPO_4^{2-}/PO_4^{3-} than the single-anion pH 12 solution, thereby reducing the amount of neighboring ammonium sites required to stabilize the anion, meaning, greater efficiency of the ACE to capture P species. However, this does not explain the lack of P capture at pH 12 for the single-anion solution. It is hypothesized that at pH 12, the ammonium groups convert back to amine groups upon the cation's reaction with OH^- after exchange with $C1^-$ at pH 12. This gives a lack of sufficient neighboring ammonium sites to stabilize the anionic PO_4^{3-} species, reducing P uptake. Cr maintained the highest uptake capacity species likely due to a complex and synergistic combination of $CrO_4^{2-} \leftrightarrow 2Cl^-$ ion-exchanges, amine oxidation-CrO_4^{2-} reduction reactions, and Cr(III)·amine/amide/imide chelation. Through Cr adsorption isotherms and XPS analysis performed on nano PEI/silica sorbents, Choi et al. found that a portion of Cr(VI) adsorbs onto $-NH_3^+$ sites through ionic interactions at low pH.[54] Parallel to this, part of the Cr(VI) reduced to Cr (III) through oxidation of the amine groups. Subsequently, Cr(III) chelated with free amines and possibly with oxidized amine species.

No discernable trend in the overall uptake of anions from the mixed solution was observed in Figure 4 (b). This could result from the conversion of $R\text{-}NH_3^+ \cdot Cl^-$ to $R\text{-}NH_2^+(C{=}O) \cdot Cl^-$ upon oxidation by chromate. Figure S3 in the SI confirms oxidation of the amines via infrared spectroscopy. A variety of protonated amines from amides with different R-groups, like R-substituted benzene and substituted pyridine, were shown to coordinate anions like Cl^- and others through ionic interactions.[55] These $R\text{-}NH_3^+ \cdot Cl^-$ to $R\text{-}NH_2^+(C{=}O) \cdot Cl^-$ species will inherently have different proton binding affinities and Cl^- coordination strengths. Broad distribution of Cl^- coordination strengths among protonated amines and amides could obscure trends in the binding affinity of the anions. It is worth mentioning, most wastewater sources targeted by the ACE will not have chromium levels reaching 5 mM. Therefore, the oxidation of amines should be only a minor factor affecting ACE anion affinity under realistic conditions. Despite the lack of predictable anion uptake behavior, the total uptake capacity of PEI-E3/S-HCl_1.1 was 1.21 mmol anion/g-sorb., translating to 2.25 mmol negative charge/g-sorb. This is close to the maximum ~2.6 mmol anion/g-sorb. capacity calculated from the potentiometric titration. Moreover, the performance values of PEI-E3/S-HCl_1.1 were close to the 1.61 mmol anion/g-sorb. and 2.54 mmol negative charge/g-sorb. values for the commercial A600E/9149 anion exchange resin.

Like the two-step HCl washed ACE, the single-step ACE were characterized then tested for metal uptake performance from the same mixed solution, as shown in Figure S4 of the SI. Resembling the IR spectra of two-step ACE (Figure 1 (a)), the spectra of single-step ACE in (a) show the distinct feature of ammonium ions (1,580 and 2,480 cm^{-1}), which strengthen as the ratio of DPX/PEI increases from 0.6 to 1.2. Consistent IR features for the ammonium-chloride ion pairs at a DPX/PEI ratio of 1 correspond to the leveling-off of the EDS Cl/N ratio profile, as shown in (b), and to an optimum 99.6% organic content retained value shown in (c). Collectively, the results reflect robust cross-linking and effective protonation of PEI by the HCl byproduct. EDS gave a Cl^- loading of 0.77±0.12 mmol Cl^-/g-sorb. for PEI-DPX/S_1.0 compared to 1.29±0.6 mmol Cl^-/g-sorb. for the two-step PEI-E3/S-HCl_1.1. Due to this 40% reduced Cl^- content, the ~54% lower total anion uptake capacity for PEI-DPX/S_1.0, shown in (d) was expected. Future work on the single-step ACE would involve improving the crosslinking efficiency of DPX and PEI or trying other amine-chlorolinker pairs, to give more ammonium-chloride pairs. Going forward, all tests were performed with the two-step ACE.

Further examining the selectivity of PEI-E3/S-HCl_1.1 for anionic critical metals, relative maximum anion uptake tests were conducted with 5 mM total of equimolar CrO_4^{2-}/SO_4^-, CrO_4^{2-}/NO_3^-, $CrO_4^{2-}/HAsO_4^{2-}$, $HAsO_4^{2-}/SO_4^{2-}$, $HAsO_4^{2-}/NO_3^-$ mixtures. Figure S5 shows the sorbent clearly preferred Cr and As over the other species often coexisting with the critical metals in natural waters. Nearly no SO_4^{2-} and NO_3^- were adsorbed, giving excessively large molar selectivity to Cr and As. When mixed, the Cr/As selectivity was 1.88. These results supplement those for the six-metal mixed solution.

3.3 Effect of pH, Temperature, and Cl^- Content on Metal Uptake

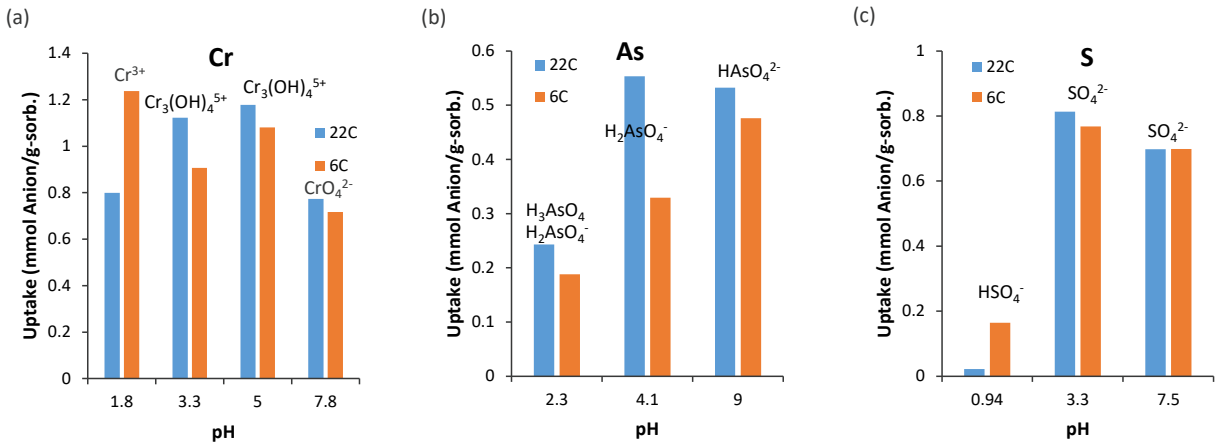

Figure 5: Effect of pH and temperature on the relative maximum uptake of (a) chromium, (b) arsenic, and (c) sulfur oxyanions by PEI-E3/S-HCl_1.1. The oxyanion(s) listed inside each figure highlight the most prevalent anion forms at each pH, according to the speciation calculations. Conditions: 0.05 g PEI-E3/S-HCl_1.1; ~5 mM total, 50 mL, 24 hours; pH 0.94-9.0; 22 °C.

Figure 5 shows the effect of initial pH and temperature on the uptake of the two critical metal oxyanions, chromate-based and arsenate-based forms, plus pervasive sulfate-based forms by PEI-E3/S-HCl_1.1. Most forms of the three oxyanions displayed slightly to moderately lower uptake

at 6 °C (refrigerated) compared to 22 °C, due to the reduced ion exchange kinetics. Speciation plots for chromium reveal that increasing the pH to 5 at 22 °C caused only a slight shift in the distribution of chromate-based species, with $HCrO_4^-$ remaining the dominant form. However, this pH increase led to a moderate enhancement in overall oxyanion uptake. Unexpectedly, the Cr Pourbaix diagram in Figure S2 showed that reduced forms of Cr as Cr^{3+} and $Cr_3(OH)_4^{5+}$ were the dominant species. This discrepancy between the speciation plot and Pourbaix diagram results from differences between the calculated and resulting Eh values. The Eh values measured by the redox probe are lower than those calculated by the PHREEQ software. The dominant species calculated from PHREEQ using the pH and Eh conditions of the solution agree with the Pourbaix diagram.

Better uptake at pH 5 at 22 °C is ascribed to lower Cl^- anion concentration (less HCl), which shifts the ion exchange equilibrium toward greater metal oxyanion adsorption. Upon raising the pH to 7.8, CrO_4^{-2} is the dominant form and gives lower mmol anion/g-sorb. uptake due to both doubling of the negative charge, which requires two ion exchange sites instead of one to capture the anion, and raising the pKa value lowering pKb/strengthening basicity. Greater pKa leads to higher hydration energies and stabilizes the CrO_4^{-2} anions in the solution, making them less prone to adsorption by the sorbent. The uptake trend at 6 °C resembled that at 22 °C, except for high uptake at pH 1.8, which was not expected. These results emphasize the importance of optimizing pH conditions to balance sorbent capacity and efficiency, given the complex interaction between ion exchange, hydration energy, and solution speciation. As uptake improved with pH as molecular, H_3AsO_4 was transformed into charged $H_2AsO_4^-$ and $HAsO_4^{2-}$ that could be captured by anion exchange at both temperatures. Gradual improvement in As uptake with rising pH at 6 °C compared to sharp improvement at 22 °C might be explained by a more rigid polymer network within the sorbent at lower temperatures, hindering access of the oxyanions to the Cl^- exchange sites.

Because anion exchange is an equilibrium process and various alkali/alkaline chloride salts are dominant species in most water systems, the effect of Cl^- concentration (as NaCl) on metal uptake was investigated. Figure 6 (a) clearly shows diminishing equilibrium uptake for each anion as the chloride content rises from 0.002 mol Cl^- (117 ppm NaCl) to 0.2 mol Cl^- (1.17 wt.% NaCl). This decline may be attributed to the shift in anion exchange equilibrium, where the excess aqueous Cl^- anions from the salt reduced the driving force for Cl^- release from PEI-E3/S-HCl_1.1. Alternatively, higher ionic strength of the solutions with greater Cl^- concentrations may have reduced the activity of the target anions. Thus, the sorbent's anion uptake capacity is limited. The sharper reduction in capacity when Cl^- concentration increases from 0.02 mol (0.17 wt.% NaCl) to 0.2 than from 0.002 to 0.02 mol indicates that more sorbent is needed for metal removal/recovery from higher salinity, contaminated wastewaters.

Figure 6 (b) shows the pH reduction caused by anion removal from solution and the addition of H^+ from the sorbent. Removal of $HAsO_4^{2-}$ likely shifted the equilibrium toward the formation of $H_2AsO_4^{-1}$, causing residual dihydrogen arsenate to deprotonate and decrease the pH approximately 1.2 units. Similarly but to a lesser extent than As removal, CrO_4^{2-} uptake decreases the pH by ~0.5 units.

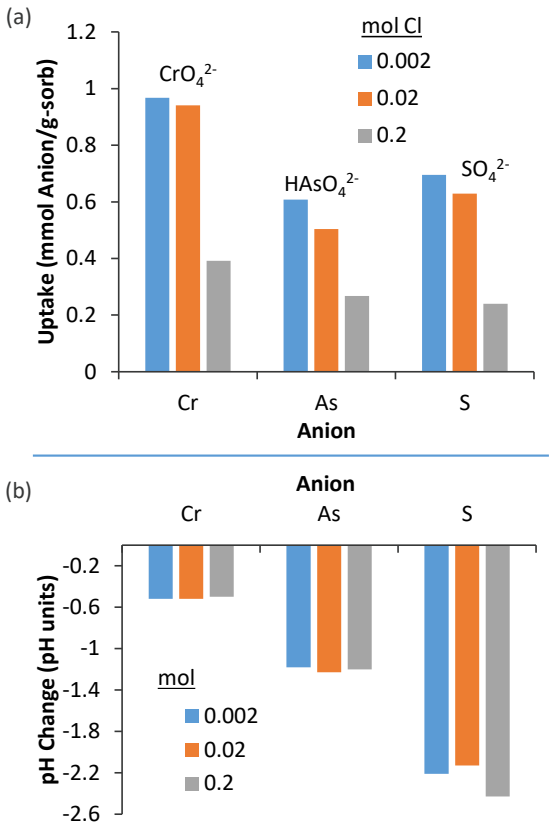

Figure 6: Effect of chloride concentration on the relative maximum uptake of Cr, As, and S species from single-anion solutions by PEI-E3/S-HCl_1.1. Starting pH values for the solutions in order of increasing Cl^- content were as follows: Conditions: 0.05 g PEI-E3/S-HCl_1.1; ~4.5-5 mM Cr, As and S, 0.002-0.2 M Cl^{-1}, 50 mL, 24 hours; pH: Cr – 8.07, 7.99, 7.79; As – 8.59, 8.52, 8.26; S – 5.64, 5.54, 5.54; 6 or 22 °C.

Removal of SO_4^{2-} caused a significant drop in pH by up to ~2.5 units instead of increasing the pH to near the level of RO water, which has negligible anionic species. This suggests that a small amount of residual HCl was rinsed from the sorbent. Overall, the results indicate that water sources with higher Cl^- content could require more sorbent to achieve the same level of anion removal as sources with lower Cl^-. Furthermore, the data suggests that the inherent pH-altering effect of the ACE could influence anion uptake, presumably by changing the anion speciation either in the bulk solution or near the sorbent's exchange sites.

3.4 Fixed-bed Breakthrough Studies

Breakthrough testing with 1 mM total, near equimolar As, Cr, and S solution at pH 7.6 was performed to probe the dynamic uptake behavior of PEI-E3/S-HCl_1.1, as shown in Figure 7. Rapid breakthrough of As, reaching approximately 1.8 normalized concentration, followed by gradual return to the inlet concentration (value of 1) signifies displacement of lower affinity As species (primarily $HAsO_4^{2-}$,) by higher affinity Cr species (primarily CrO_4^{2-}), which did not breakthrough until the final few mL's of the run.

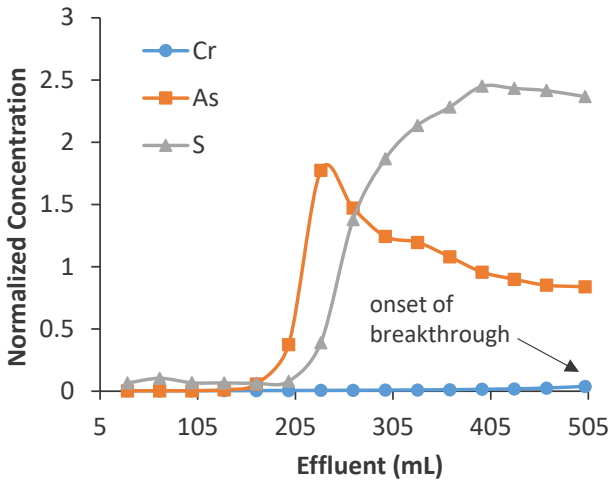

Figure 7: Normalized uptake profiles during breakthrough testing of ACE with Cr, As, and S. Profiles for the anions were normalized to their inlet concentrations. Conditions: 0.5 g PEI-E3/S-HCl_1.1; 1.0 mM total, equimolar anions, 500 mL, 0.5 mL/min; and pH 7.6; 22 °C.

Displacement of a greater portion of adsorbed S relative to adsorbed As was indicated by the rapid then gradual jump in the S normalized concentration up to 2.4. Similar metal concentration spikes, surpassing the inlet values, have been observed in other mixed metal adsorption tests, indicting weaker binding of the metals to the sorbent.[56] Meaning, the weakly bound metals were displaced by those more strongly bound. Contrasting the As profile, which decreased quickly, the S profile displayed a sluggish decline. This behavior may result from either diffusion-limited release of S from the internal ACE pore structure or further S desorption owed to re-adsorption of previously desorbed As. The largest breakthrough volume for Cr, onset at 500 mL, signifies the greatest affinity of the sorbent for chromate. This was previously forecasted by the relative maximum uptake data for the six-anion mixed solution.

It is worth mentioning that although the arsenate-sulfate breakthrough tests in the literature and this work reveal higher affinity for sulfate than arsenate under more ideal conditions, the results presented in Figures 4, 5, and 6 highlight that mixed anions, pH, and chloride content all affect anion uptake preferences. One study even showed that an increase in the ratio of aqueous sulfate/chromate increased chromate selectivity of an ion exchange resin due to partial dehydration of the resin.[57] Predicated on these observations, it is recommended that the performance of a sorbent to clean wastewaters is best assessed by testing more complex systems, or ideally authentic waste water.

Breakthrough testing with 2 mM equimolar solution containing P, As, Br^-, NO_3^-, Se, and SO_4^{2-}, without Cr, shown in Figure 8, showcases the sorbent's anion uptake primarily through ion exchange with minimal influence from oxidation-reduction reactions. Dramatic breakthrough of NO_3^- and Br^- (lowest pKa's tested), reaching ~2.9 and ~2.5 normalized concentration, respectively, plotted in (a) reflect significant displacement by more strongly adsorbed P and As anions. These anions, with the highest pKa's tested, broke through in (c) shortly after NO_3^- and Br^- and reached ~1.6 normalized concentration. However, the amount of desorbed NO_3^- and Br^- was disproportionately higher than the amount of incoming P/As causing displacement. This suggests

that an additional anion more strongly bound than P or As to the exchange sites is present and contributing to the excessive NO_3^- and Br^- displacement.

SO_4^{2-} and Se broke through later in the adsorption process, indicting their initial higher uptake by the sorbent. These anions were subsequently desorbed or displaced, reflective of their >1 normalized concentration values. These kinetic results align with the batch equilibrium uptake results presented in Figure S6 for a 5 mM equimolar analogous solution. Results showed that the ACE captured no NO_3^-, Br^-, and SO_4^{2-} after the 24-hour uptake test. These anions were presumably displaced early on by HPO_4^{2-}, $HAsO_4^{2-}$, and SeO_4^{2-} which were preferentially captured by the sorbent.

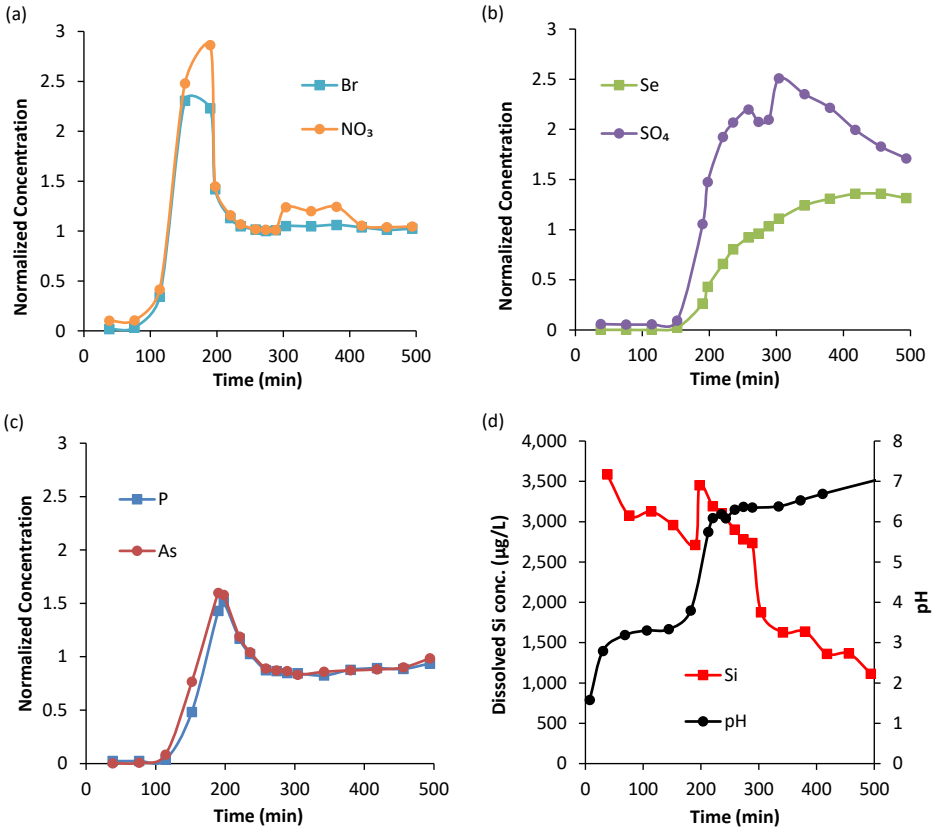

Figure 8: Effluent normalized concentration profiles during breakthrough testing with a 6-anion mixed solution, containing (a) Br^-, NO_3^-; (b) S, Se; (c) P, As. (d) Si released into solution from dissolved SiO_2, and effluent pH value. Profiles for the anions were normalized to their inlet concentrations. Conditions: 0.5 g PEI-E3/S-HCl_1.1; ~2.0 mM total, equimolar anions, 500 mL, 0.5 mL/min; pH 10.5; 22 °C.

Dissolution of silica under acidic and basic conditions produced silicic acid monomers, $Si(OH)_4$ with pKa ~9.5, and a collection of oligomers.[58-60] Alternative to dissolution, silica could deteriorate from larger agglomerates to smaller nanosized particles whose surface functional groups could exhibit pKa values from ~2 to ~16.[61] It is reasonable that a distribution of silicic acid species, having a broad range of pKa values, competed with the oxyanions targeted in this study for anion binding sites. Figure 8 (d) shows an overall diminishing release of soluble Si from the ACE particles into solution, with two notable exceptions: between 180-190 (pH 3.3-3.8) and 289 (pH 6.4) min, where the Si profile rises sharply in parallel with pH. Results of an overnight silica dissolution experiment, shown in Figure S7, exhibited a jump in dissolved Si concentration upon

going from initial pH 3 to initial pH 6. The results suggest that the release of soluble Si is pH dependent. Thereby, increased Si dissolution occurred during the specific pH shift observed while flow testing. Additionally, treatment of PEI-ES/S-HCl_1.1 with pH 2.9 HCl (no metals) generated <0.18 ppm (below detection limit, BDL) dissolved Si species as shown in Table S4. Minimal loss of these species was associated with less than 15% changes in the BET surface area (4.3% increase), BJH pore volume, and BJH average pore size. Treatment with pH 1.2 also generated BDL Si; produced little change in SA; but increased pore volume and average pore size by 20-25%. These results suggest a displacement/exchange effect only during metal uptake testing, whereby contaminant metals replace Si within the silica matrix instead of simple Si dissolution under low pH conditions.

An inlet solution pH of 10.5 for the flow test points to base-catalyzed silica dissolution at the point of first contacting the sorbent bed to form anionic silicate species that displaced the other downstream-adsorbed target oxyanions. One study found that 30 ppm dissolved Si dramatically diminished the uptake of targeted As (few hundred ppb) by ArsenX^{np} anion exchange resin modified with iron hydroxide nanoparticles as the pH increased from 7.2 to 9.0. This behavior was due to enhanced dissociation of silica into conjugate base anionic oligomers that outcompeted As for the binding sites.[62]

The concentration of Si in the ACE-treated effluent solution was low and steadily decreasing, and silica is not regulated by the EPA. Therefore, the presence of silica only becomes a concern when aqueous CMs are at low ppb levels relative to high ppm silica, or when high purities of recovered CMs are desired. Removal of Si can be achieved through precipitation via pH adjustment prior to treatment with ACE, either alone or in combination with a salt such as $CaCl_2$ to form insoluble calcium silicate.[63] Alternatively, silica species co-precipitated with the CM released from the ACE during elution can be subsequently dissolved in alkaline solution. This leaves the solid precipitated CM behind.

Acidic solutions exiting the ACE bed necessitated a pH gradient through the sorbent and possibly a concentration gradient of mixed oxyanion species according to the structures calculated in Figure S1. This gradient helps explain the difference among the oxyanion breakthrough profiles, where competing adsorption-desorption kinetics along the gradient would affect the profiles' relative shapes. Both the rates of oxyanion protonation-deprotonation and the sorbent-solution contact time underpin any gradient of species across the sorbent bed. These results further strengthen the necessity to use an authentic wastewater sample to assess and optimize the uptake performance of a candidate sorbent for a target water source.

Flue gas desulfurization wastewater (ix) is highly mineralized with Ca^{2+}, Mg^{2+}, Na^{+}, and many of the oxyanions (e.g., As, Cr, P, N, and Se) found in the ideal solutions are tested in this work, as shown in Tables S1 and S3. Sorbents previously tested in the literature for FGD clean-up include: hexadecyltrimethylammonium bromide-modified zeolite;[64] polyethylenimine-n,n'-methylenebisacrylamide-functionalized silica (our previous work);[7] chitosan-modified zirconium;[65] and combinations of different commercial chelating resins.[66] Industrial application of sorbents, such as commercialized ion exchange resins, mandates their regenerability to avoid steep material costs for the overall treatment/recovery process. Surprisingly, anion exchange sorbents are scarcely reported for FGD wastewater clean-up.

3.5 Authentic Coal Wastewater Treatment

Figure 9 shows the contaminant adsorption-desorption performance of PEI-E3/S-HCl_1.1 over 8 cycles. Testing 1 M (20 mL total), 1 M (40 mL total), and 3 M (20 mL total) NaCl (not shown) revealed that a single 1 M NaCl rinse was sufficient to desorb most of the adsorbed anions. A 1.5 g bed of ACE was determined sufficient to appreciably treat 20 mL FGD due to the high anion concentrations, as shown in Figure S8 (a).

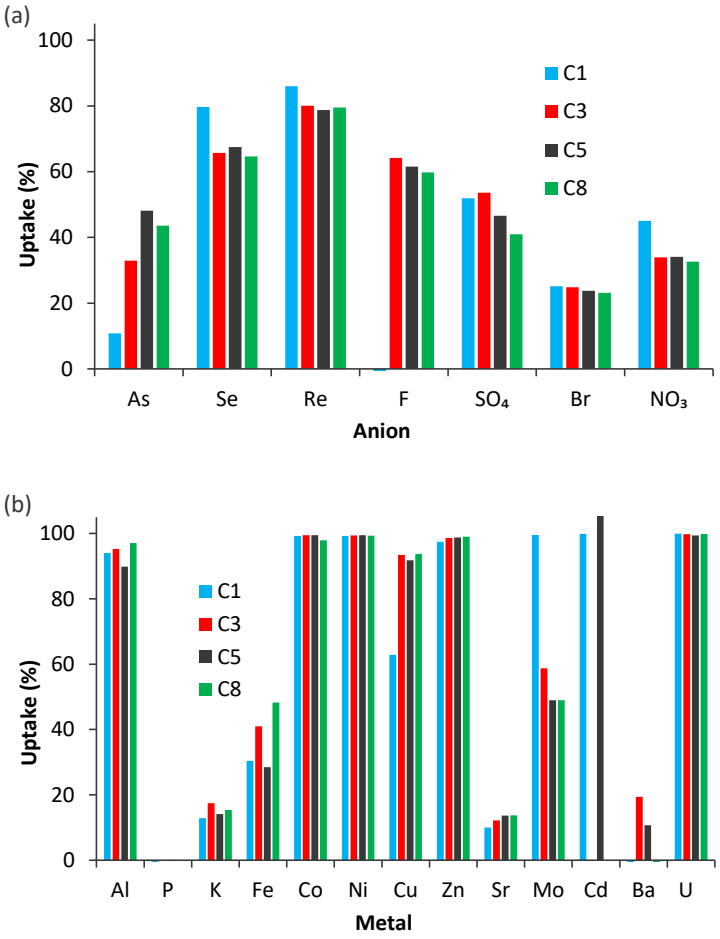

Figure 9: Cyclic contaminant uptake performance of PEI-E3/S-HCl_1.1 when treating authentic FGD wastewater (ix). Conditions: 1.5 g PEI-E3/S-HCl_1.1; 20 mL FGD (metal removal) or 1 wt.% NaCl (metal release), 0.5 mL/min flow rate; and pH 6.9; 22 °C.

The percent uptake varied across the anions as follows: Re (presumably ReO_4^-)>Se, F^->SO_4^{2-}, As, and NO_3^->Br^-. Uptake of these contaminants from FGD were predicted from the results presented in Figure 8 for treating the ideal mixed anion solution. However, the drastically different chemistries of the two waters gave dissimilar anion uptake trends between the tests. After cycle 1, the uptake percent of most anions from FGD either maintained or gradually decreased down to cycle 8, except for As which significantly increased. Interestingly, the ACE consistently removed cationic Al, Co, Ni, Cu, Zn, and U, highlighting utilization of the remaining non-protonated free amines inferred from the potentiometric titration and EDS data.

The performance of two, 1.5 g beds of ACE for treating 20 mL of the (ix) FGD was compared against the same amounts of other commercial sorbents, including the A600E/9149 resin and others, and is illustrated in Figure S8 (b). The results revealed that PEI-E3/S-HCl_1.1 adsorbed an appreciable amount of the contaminants relative to the other sorbents, showing that ACE could compete with these materials in the marketplace. Treating another authentic FGD wastewater sample (x) spiked with Cr and As but cleaner than (ix), shown in Figure S9 of the SI, reveals similar uptake of Cr and NO_3^- and higher As, Se, F, and SO_4^{2-} uptake for PEI-E3/S-HCl_1.1 when comparing ACE to the A600E/9149 resin, respectively.

Further exploring the potential of the two-step ACE to clean contaminated waters, pH 3.5 coal ash leachate originating from the Powder River Basin in Wyoming, USA was tested. The composition of the solution is shown in Table S5. As shown in Figure S10, treatment with 0.5 g of PEI-E3/S-HCl_1.1 removed 73% of the initial 564 mg/L SO_4^{2-}; 21% of 43 mg/L Si (likely silicate monomers); 96% of 2.6 µg/L Mo (likely molybdate) from 20 mL of leachate, while Cr (321 µg/L), As (14.5 µg/L), and Se (28.5 µg/L) were not removed. This contrasts with the clear removal of As and Se from the FGD, which is at higher pH but higher Cl^- concentration than those of the leachate. Although lower Cl^- concentration in the leachate should theoretically provide greater driving force for As and Se anion exchange, the lower pH may lead to stronger -NH_3^+/-$NH_2^+\cdots Cl^-$ ionic bonding and increased charge-charge repulsion between ammonium ions and H_3O^+. In contrast, the higher pH of the FGD wastewater could weaken the immobilized ammonium chloride species through -$OH^-\cdots$-NH_3^+/-NH_2^+ interactions, thereby facilitating anion exchange with the contaminants.

Overall, the ACE demonstrated good-to-excellent anion uptake between pH 2.4 and 8.5. Practical application of the two-step ACE sorbent was demonstrated by removing toxic and/or valuable species from multiple authentic contaminated wastewater sources. Optimizing the uptake parameters at lab scale would be required prior to scale-up testing of each solution given their different compositions.

4 CONCLUSIONS

Functionalized silica ACE sorbents were developed using two different approaches: (1) acid washing epoxy-crosslinked, immobilized amine sorbents for two-step formulas; and (2) using a di-chlorinated crosslinker/amine combination for single-step formulas. The best performing, optimized two-step PEI-E3/S-HCl_1.1 removed toxic or nuisance oxyanionic As, Cr, Se, P, S (SO_4^{2-}), and N (NO_3^-) species plus Br^- from both ideal solutions and authentic AMD and FGD wastewaters. Excitingly, the ACE exhibited a high uptake of 2.25 mmol negative charge/g-sorb. that was close to the 2.54 mmol negative charge/g-sorb. of a commercial anion exchange resin.

EDS and DRIFTS analyses confirmed the presence of the exchangeable Cl^- groups responsible for anion removal, where those for Cr, As, and S were appreciably diminished only at a higher 0.2 M Cl^- (as NaCl) concentration. Effective uptake of these anions at room temperature and low groundwater temperature (6 °C) under both acidic and basic conditions predicted successful practical application of ACE. Although the sorbent demonstrated the highest affinity for Cr, it successfully cleaned many contaminant species from authentic FGD even better than the commercial resin. Furthermore, the ACE consistently removed between 25% and 80% of all tested anions from the FGD during eight-cycle testing. Overall, the results of this work demonstrate the

viability of the ACE sorbent to effectively recover/remove critical/toxic anions under practical conditions, justifying future scale-up studies to further explore and optimize the sorbents' practical applications. Further optimization of the ACE may give better performance than the commercial resin when treating different other ideal and authentic wastewaters.

5 ASSOCIATED CONTENT

Supporting Information.

The following files are available free of charge. Word document containing the following data: table of solution compositions; infrared spectra of fresh and Cr-adsorbed ACE; anion uptake from a mixture containing P, As, Se, S, Br^-, and NO_3^-; effect of pH on the dissolution of silica; comparison among 0.5-1.5 g PEI-E3/S-HCl_1.1 and among different sorbents for anion removal from FGD; comparing different sorbents for anion uptake from a second authentic sample of FGD wastewater at different pH values; and table listing the properties of different commercial anion exchange sorbents.

6 AUTHOR INFORMATION

Corresponding Author

Walter Chris Wilfong* – Walter.Wilfong@netl.doe.gov

Author Contributions

The manuscript was written through contributions of all authors. All authors have given approval to the final version of the manuscript. All authors contributed equally.

Funding Sources

This work was performed in support of the U.S. Department of Energy's (DOE) Office of Fossil Energy and Carbon Management's Minerals Sustainability Program and executed through the National Energy Technology Laboratory (NETL) Research & Innovation Center's Minerals Sustainability Multi-Year Research Plan.

7 ACKNOWLEDGMENT

We thank Nicholas Siefert for providing samples of authentic FGD wastewater.

8 DISCLAIMER

This project was funded by the United States Department of Energy, National Energy Technology Laboratory, in part, through a site support contract.

9 ABBREVIATIONS

ACE – ammonium-coordinated exchanger; RCRA – Resource Conservation and Recovery Act; EPA – U.S. Environmental Protection Agency; AMD – acid mine drainage; FGD – flue gas desulfurization wastewater; PEI – polyethylenimine; E3 – N,N-diglycidyl-4-glycidyloxyaniline; DPX – α, α-dichloro-p-xylene; ICP-MS – inductively coupled plasma-mass spectrometry; IC – ion chromatography; ICP-OES – inductively coupled plasma-optical emission spectroscopy; Uv-Vis – ultraviolet-visible light (spectroscopy); DRIFTS – diffuse reflectance infrared Fourier transform spectroscopy; MeOH – methanol; TGA – thermogravimetric analysis; SEM – scanning electron microscopy; EDS – energy-dispersive X-ray spectroscopy; CHNS – carbon-hydrogen-nitrogen-sulfur (analysis); CVAAS – cold vapor atomic absorption spectroscopy; BDL – below detection limit.

10 REFERENCES

1. United States National Archives and Records Administration, Code of Federal Regulations, 40 CFR § 268.40 - Applicability of treatment standards, https://www.ecfr.gov/current/title-40/chapter-I/subchapter-I/part-268/subpart-D. (accessed 10/14/2024).
2. Waters, W. A., Mechanisms of oxidation by compounds of chromium and manganese. *Quarterly Reviews, Chemical Society* **1958,** *12* (4), 277-300.
3. Carrington, A.; Symons, M. C. R., Structure and Reactivity of the Oxyanions of Transition Metals. *Chemical Reviews* **1963,** *63* (5), 443-460.
4. Tsai, S.-L.; Singh, S.; Chen, W., Arsenic metabolism by microbes in nature and the impact on arsenic remediation. *Current Opinion in Biotechnology* **2009,** *20* (6), 659-667.
5. Peak, D.; Sparks, D., Mechanisms of selenate adsorption on iron oxides and hydroxides. *Environmental science & technology* **2002,** *36* (7), 1460-1466.
6. United States Geological Survey, Mineral Commodity Summaries 2024, Estimated United States Salient Critical Minerals Statistics in 2023. https://tableau.usgs.gov/views/MCSDashboardWorkbook_2024-01-30/MCSDashboard?%3Aembed=y&%3AisGuestRedirectFromVizportal=y#7. (accessed 10/14/2024).
7. Wang, Q.; Wilfong, W.; Kail, B.; Ji, T.; Shi, F.; Gray, M., Effective removal of trace-level toxic metals from flue gas desulfurization wastewater using SiO2 supported hydrogel sorbent. *Materials Today Sustainability* **2023,** *21*, 100324.
8. Bednar, A. J.; Garbarino, J. R.; Ranville, J. F.; Wildeman, T. R., Preserving the Distribution of Inorganic Arsenic Species in Groundwater and Acid Mine Drainage Samples. *Environmental Science & Technology* **2002,** *36* (10), 2213-2218.
9. United Dtates Enviromental Protection Agency, Nutrient Pollution - The Sources and Solutions: Agriculture. https://www.epa.gov/nutrientpollution/sources-and-solutions-agriculture (accessed 4/24/2023).
10. Marinho, B. A.; Cristóvão, R. O.; Boaventura, R. A. R.; Vilar, V. J. P., As(III) and Cr(VI) oxyanion removal from water by advanced oxidation/reduction processes—a review. *Environmental Science and Pollution Research* **2019,** *26* (3), 2203-2227.
11. Rezvani, F.; Sarrafzadeh, M.-H.; Ebrahimi, S.; Oh, H.-M., Nitrate removal from drinking water with a focus on biological methods: a review. *Environmental Science and Pollution Research* **2019,** *26* (2), 1124-1141.

12. Runtti, H.; Tolonen, E.-T.; Tuomikoski, S.; Luukkonen, T.; Lassi, U., How to tackle the stringent sulfate removal requirements in mine water treatment—A review of potential methods. *Environmental Research* **2018,** *167*, 207-222.
13. Veolia, Ion Exchange Systems - High purity softened and demineralized water. https://www.watertechnologies.com/products/ion-exchange. (accessed 11/13/2024).
14. Pandey, S.; Mishra, S. B., Organic–inorganic hybrid of chitosan/organoclay bionanocomposites for hexavalent chromium uptake. *Journal of Colloid and Interface Science* **2011,** *361* (2), 509-520.
15. Hérès, X.; Blet, V.; Di Natale, P.; Ouaattou, A.; Mazouz, H.; Dhiba, D.; Cuer, F., Selective extraction of rare earth elements from phosphoric acid by ion exchange resins. *Metals* **2018,** *8* (9), 682.
16. PQ Corporation, Product data sheet - ADVERA® Specialty Zeolites. https://www.pqcorp.com/products/zeolites/advera. (accessed 3/10/2021.
17. Sublet, R.; Simonnot, M.-O.; Boireau, A.; Sardin, M., Selection of an adsorbent for lead removal from drinking water by a point-of-use treatment device. *Water Research* **2003,** *37* (20), 4904-4912.
18. Lanxess, Product Infortmation - Lewatit FO 36, https://www.lenntech.com/Data-sheets/Lewatit-FO-36-L.pdf. (accessed 10/14/2024).
19. Wilfong, W. C.; Wang, Q.; Shi, F.; Howard, B.; Gray, M., Multi-functional Sorbent Technology (MUST) for the Recovery/Removal of Critical/Heavy Metals from Fossil-Related Wastewater. *2024 Spring Meeting and 20th Global Congress on Process Safety Location: New Orleans, LA, United States*.
20. Wang, Q.; Kail, B. W.; Wilfong, W. C.; Shi, F.; Tarka, T. J.; Gray, M. L., Amine Sorbents for Selective Recovery of Heavy Rare-Earth Elements (Dysprosium, Ytterbium) from Aqueous Solution. *ChemPlusChem* **2020,** *85* (1), 130-136.
21. Zhao, F.; Repo, E.; Song, Y.; Yin, D.; Hammouda, S. B.; Chen, L.; Kalliola, S.; Tang, J.; Tam, K. C.; Sillanpää, M., Polyethylenimine-cross-linked cellulose nanocrystals for highly efficient recovery of rare earth elements from water and a mechanism study. *Green Chemistry* **2017,** *19* (20), 4816-4828.
22. Ramasamy, D. L.; Khan, S.; Repo, E.; Sillanpää, M., Synthesis of mesoporous and microporous amine and non-amine functionalized silica gels for the application of rare earth elements (REE) recovery from the waste water-understanding the role of pH, temperature, calcination and mechanism in Light REE and Heavy REE separation. *Chemical Engineering Journal* **2017,** *322*, 56-65.
23. Florek, J.; Lariviere, D.; Kahlig, H.; Fiorilli, S. L.; Onida, B.; Fontaine, F. G.; Kleitz, F., Understanding Selectivity of Mesoporous Silica-Grafted Diglycolamide-Type Ligands in the Solid-Phase Extraction of Rare Earths. *ACS Appl Mater Interfaces* **2020,** *12* (51), 57003-57016.
24. Hu, Y.; Misal Castro, L. C.; Drouin, E.; Florek, J.; Kählig, H.; Larivière, D.; Kleitz, F.; Fontaine, F.-G., Size-Selective Separation of Rare Earth Elements Using Functionalized Mesoporous Silica Materials. *ACS Applied Materials & Interfaces* **2019,** *11* (26), 23681-23691.
25. Roosen, J.; Spooren, J.; Binnemans, K., Adsorption performance of functionalized chitosan–silica hybrid materials toward rare earths. *J. Mater. Chem. A* **2014,** *2* (45), 19415-19426.
26. Li, J.; Gong, A.; Qiu, L.; Zhang, W.; Shi, G.; Li, X.; Li, J.; Gao, G.; Bai, Y., Selective extraction and column separation for 16 kinds of rare earth element ions by using N, N-

dioctyl diglycolacid grafted silica gel particles as the stationary phase. *J Chromatogr A* **2020,** *1627*, 461393.
27. Zheng, X.; Song, Z.; Liu, E.; Zhang, Y.; Li, Z., Preparation of Phosphoric Acid-Functionalized SBA-15 and Its High Efficient Selective Adsorption Separation of Lanthanum Ions. *Journal of Chemical & Engineering Data* **2020,** *65* (2), 746-756.
28. Tundo, P.; Venturello, P.; Angeletti, E., Anion-exchange properties of ammonium salts immobilized on silica gel. *Journal of the American Chemical Society* **1982,** *104* (24), 6547-6551.
29. Chen, L.; Yin, X.; Yu, Q.; Siming, L.; Meng, F.; Ning, S.; Wang, X.; Wei, Y., Rapid and selective capture of perrhenate anion from simulated groundwater by a mesoporous silica-supported anion exchanger. *Microporous and Mesoporous Materials* **2019,** *274*, 155-162.
30. Hamoudi, S.; Belkacemi, K., Adsorption of nitrate and phosphate ions from aqueous solutions using organically-functionalized silica materials: Kinetic modeling. *Fuel* **2013,** *110*, 107-113.
31. Zhu, L.; Zhang, C.; Liu, Y.; Wang, D.; Chen, J., Direct synthesis of ordered N-methylimidazolium functionalized mesoporous silica as highly efficient anion exchanger of Cr (VI). *Journal of Materials Chemistry* **2010,** *20* (8), 1553-1559.
32. McNeff, C.; Zhao, Q.; W. Carr, P., High-performance anion exchange of small anions with polyethyleneimine-coated porous zirconia. *Journal of Chromatography A* **1994,** *684* (2), 201-211.
33. Grochowicz, M.; Gawdzik, B.; Jaćkowska, M.; Buszewski, B., Investigation of the thermal behavior of new silica-polymer anion exchangers. *Journal of Thermal Analysis and Calorimetry* **2013,** *112* (2), 885-891.
34. Wu, M.; Wu, R. a.; Wang, F.; Ren, L.; Dong, J.; Liu, Z.; Zou, H., "One-Pot" Process for Fabrication of Organic-Silica Hybrid Monolithic Capillary Columns Using Organic Monomer and Alkoxysilane. *Analytical Chemistry* **2009,** *81* (9), 3529-3536.
35. Humelnicu, D.; Ignat, M.; Dinu, M. V.; Dragan, E. S., Optimization of Arsenic Removal from Aqueous Solutions Using Amidoxime Resin Hosted by Mesoporous Silica. *ACS Omega* **2022,** *7* (35), 31069-31080.
36. Dragan, E. S.; Humelnicu, D., Contribution of Cross-Linker and Silica Morphology on Cr(VI) Sorption Performances of Organic Anion Exchangers Embedded into Silica Pores. *Molecules* **2020,** *25* (5), 1249.
37. Wilfong, W. C.; Kail, B. W.; Gray, M. L., Rapid Screening of Immobilized Amine CO2 Sorbents for Steam Stability by Their Direct Contact with Liquid H2 O. *ChemSusChem* **2015,** *8* (12), 2041-5.
38. Wilfong, W. C.; Kail, B. W.; Wang, Q.; Gray, M. L., Novel Rapid Screening of Basic Immobilized Amine Sorbent/Catalyst Water Stability by a UV/Vis/Cu(2+) Technique. *ChemSusChem* **2018,** *11* (23), 4114-4122.
39. Wilfong, W. C.; Kail, B. W.; Wang, Q.; Shi, F.; Shipley, G.; Tarka, T. J.; Gray, M. L., Stable immobilized amine sorbents for heavy metal and REE removal from industrial wastewaters. *Environmental Science: Water Research & Technology* **2020,** *6* (5), 1286-1299.
40. Gray, M. L.; Soong, Y.; Champagne, K. J.; Baltrus, J.; Stevens Jr, R. W.; Toochinda, P.; Chuang, S. S. C., CO2 capture by amine-enriched fly ash carbon sorbents. *Separation and Purification Technology* **2004,** *35* (1), 31-36.
41. Tumuluri, U.; Isenberg, M.; Tan, C. S.; Chuang, S. S., In Situ Infrared Study of the Effect of Amine Density on the Nature of Adsorbed CO2 on Amine-Functionalized Solid Sorbents. *Langmuir* **2014,** *30* (25), 7405-13.

42. Yu, J.; Chuang, S. S. C., The Structure of Adsorbed Species on Immobilized Amines in CO2 Capture: An in Situ IR Study. *Energy & Fuels* **2016,** *30* (9), 7579-7587.
43. Yu, J.; Chuang, S. S. C., The Role of Water in CO2 Capture by Amine. *Industrial & Engineering Chemistry Research* **2017**.
44. Suh, J.; Paik, H. J.; Hwang, B. K., Ionization of Poly(ethylenimine) and Poly(allylamine) at Various pH′s. *Bioorganic Chemistry* **1994,** *22* (3), 318-327.
45. Pittman Jr, C. U.; He, G. R.; Wu, B.; Gardner, S. D., Titration of tetraethylenepentamine (TEPA) and its phenyl isocyanate reaction products: A model correction factor for determination of TEPA grafted to carbon surfaces. *Carbon* **1997,** *35* (3), 333-340.
46. Grenda, K.; Idström, A.; Evenäs, L.; Persson, M.; Holmberg, K.; Bordes, R., An analytical approach to elucidate the architecture of polyethyleneimines. *Journal of Applied Polymer Science* **2022,** *139* (7), 51657.
47. Snoeyink, V. L.; Weber, W. J., The surface chemistry of active carbon; a discussion of structure and surface functional groups. *Environmental Science & Technology* **1967,** *1* (3), 228-234.
48. LibreTexts Chemistry, CRC Handbook of Chemistry and Physics, 84th Edition (2004), E1: Acid Dissociation Constants at 25°C. https://chem.libretexts.org/Ancillary_Materials/Reference/Reference_Tables/Equilibrium_Constants/E1%3A_Acid_Dissociation_Constants_at_25C. (accessed 7/25/2024).
49. Chu, B.; Whitney, D. C.; Diamond, R. M., On anion-exchange resin selectivities. *Journal of Inorganic and Nuclear Chemistry* **1962,** *24* (11), 1405-1415.
50. Abramov, A. A.; Dzhigirkhanov, M. S. A.; Iofa, B. Z.; Volkova, S. V., Hydration and Extraction of Oxyanions. *Radiochemistry* **2002,** *44* (3), 270-273.
51. Carey, F. A., *Organic Chemistry*. 5 ed.; Kent A. Peterson: New York, 2003; p 1191.
52. McNeff, C.; Carr, P. W., Synthesis and Use of Quaternized Polyethylenimine-Coated Zirconia for High-Performance Anion-Exchange Chromatography. *Analytical Chemistry* **1995,** *67* (21), 3886-3892.
53. Darmograi, G.; Prelot, B.; Geneste, A.; De Menorval, L.-C.; Zajac, J., Removal of three anionic orange-type dyes and Cr(VI) oxyanion from aqueous solutions onto strongly basic anion-exchange resin. The effect of single-component and competitive adsorption. *Colloids and Surfaces A: Physicochemical and Engineering Aspects* **2016,** *508*, 240-250.
54. Choi, K.; Lee, S.; Park, J. O.; Park, J.-A.; Cho, S.-H.; Lee, S. Y.; Lee, J. H.; Choi, J.-W., Chromium removal from aqueous solution by a PEI-silica nanocomposite. *Scientific Reports* **2018,** *8* (1), 1438.
55. Kang, S. O.; Begum, R. A.; Bowman-James, K., Amide-based ligands for anion coordination. *Angewandte Chemie International Edition* **2006,** *45* (47), 7882-7894.
56. Chiavola, A.; D'Amato, E.; Baciocchi, R., Ion Exchange Treatment of Groundwater Contaminated by Arsenic in the Presence of Sulphate. Breakthrough Experiments and Modeling. *Water, Air, & Soil Pollution* **2012,** *223* (5), 2373-2386.
57. Sengupta, A. K.; Clifford, D., Important process variables in chromate ion exchange. *Environmental Science & Technology* **1986,** *20* (2), 149-155.
58. Nangia, S.; Garrison, B. J., Reaction rates and dissolution mechanisms of quartz as a function of pH. *J Phys Chem A* **2008,** *112* (10), 2027-33.
59. Exley, C.; Guerriero, G.; Lopez, X., Silicic acid: The omniscient molecule. *Science of The Total Environment* **2019,** *665*, 432-437.

60. Dietzel, M., Dissolution of silicates and the stability of polysilicic acid. *Geochimica et Cosmochimica Acta* **2000,** *64* (19), 3275-3281.
61. Pfeiffer-Laplaud, M.; Costa, D.; Tielens, F.; Gaigeot, M.-P.; Sulpizi, M., Bimodal Acidity at the Amorphous Silica/Water Interface. *The Journal of Physical Chemistry C* **2015,** *119* (49), 27354-27362.
62. Möller, T.; Sylvester, P., Effect of silica and pH on arsenic uptake by resin/iron oxide hybrid media. *Water Research* **2008,** *42* (6), 1760-1766.
63. Kang, J.; Sun, W.; Hu, Y.; Gao, Z.; Liu, R.; Zhang, Q.; Liu, H.; Meng, X., The utilization of waste by-products for removing silicate from mineral processing wastewater via chemical precipitation. *Water Research* **2017,** *125*, 318-324.
64. Solińska, A.; Bajda, T., Modified zeolite as a sorbent for removal of contaminants from wet flue gas desulphurization wastewater. *Chemosphere* **2022,** *286*, 131772.
65. Kluczka, J., Removal of Boron and Manganese Ions from Wet-Flue Gas Desulfurization Wastewater by Hybrid Chitosan-Zirconium Sorbent. *Polymers* **2020,** *12* (3), 635.
66. Czupryński, P.; Płotka, M.; Glamowski, P.; Żukowski, W.; Bajda, T., An assessment of an ion exchange resin system for the removal and recovery of Ni, Hg, and Cr from wet flue gas desulphurization wastewater-a pilot study. *RSC Adv* **2022,** *12* (9), 5145-5156.

Abstract Graphic

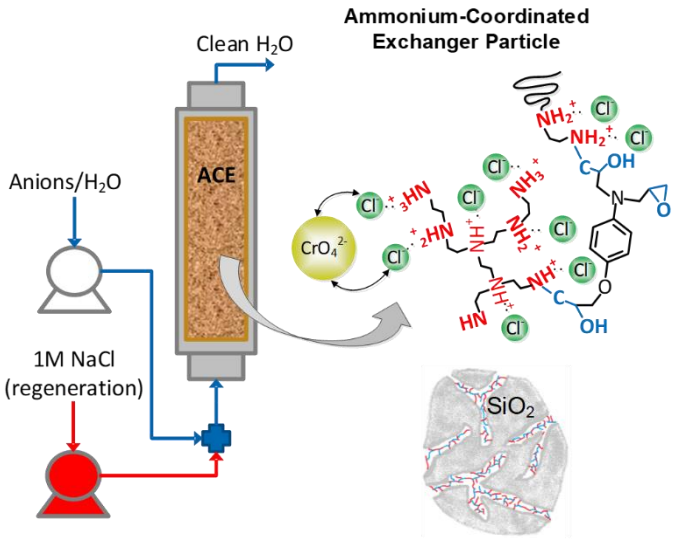
Ammonium-Coordinated
Exchanger Particle
Clean H_2O
Anions/H_2O
ACE
1M NaCl
(regeneration)
CrO_4^{2-}
SiO_2

CORRECTION TO:

Ammonium-Coordinated Exchanger (ACE) Functionalized Silica Sorbents for Recovering/Removing Aqueous Anionic Contaminants

Walter Chris Wilfong[a,b]; Qiuming Wang[a,b]; Fan Shi[a]; Chin-Min Cheng[a,b]; William Garber[a,b]; Karen Johnson[a,b]; Phillip Tinker[a,b]; Gita Bhandari[a,b]; Bret Howard[a]; McMahan L. Gray[a]**

[a]National Energy Technology Laboratory, 626 Cochran Mill Road, Pittsburgh, PA 15236, USA

[b]NETL Support Contractor, 626 Cochran Mill Road, Pittsburgh, PA 15236, USA